Experimental and Theoretical Studies of the Inhibition Effects of 4-Hydroxycoumarin Derivatives on the Corrosion of Al in Hydrochloric Acid Solution

A. S. Fouda[1,*], S. H. Etaiw[2], M. Salah[1]

[1] Department of Chemistry, Faculty of Science, El-Mansoura University, El-Mansoura-35516, Egypt,
[2] Department of Chemistry, Faculty of Science, Tanta University, Tanta, Egypt
[*]E-mail: asfouda@hotmail.com, asfouda@mans.edu.eg

The effect of 4-Hydroxycoumarin Derivatives (HCD), as a safe inhibitor, was examined by calculating the corrosion of Al in 1.0 M HCl solution at 25–45°C. Calculation was shown under numerous experimental conditions utilized mass loss (ML), Tafel polarization (TP), electrochemical impedance EIS and electrochemical frequency modulation EFM tests. The protection efficiency (% I) improved with raised in concentration of the inhibitors. Rise in temperature improved the corrosion rate in the existence and nonexistence of inhibitors but reduced the protection efficiency. (HCD) obeyed adsorption isotherm of Langmuir at all temperatures used. TP curves gave indication that the HCD act as mixed-kind inhibitor. The morphology of inhibited Al surface was analyzed by scanning electron microscope (SEM), Fourier transform infrared spectroscopy (FTIR) and nanotechnology atomic force microscopy (AFM). Finally, Theoretical data and experimental results were in good correlation.

1. INTRODUCTION

Corrosion of Al and its alloys has been the focus on several research due to their significance and using in various manufacturing, such as pipes, machinery, and reaction vessels, due to their benefits such as thermal conductivity and lightness. However, in spite of its significance, it is therefore commanding to add corrosion inhibitors to reduction the rate of corrosion of Al in aqueous solutions [1-3]. HCl is extensively utilizing in acid pickling, acid cleaning and oil well acidizing. Therefore, it is a significant to utilized corrosion protection to lower metal liquefaction. The most common method for corrosion protection of metals especially in acidic media is the using of inhibitors. Most of inhibitors used are organic, consisting of nitrogen and oxygen atoms that are highly inhibited and easily

produced [4]. These inhibitors are used to prevent the corrosion of Fe, Al and Cu in the various corroding media because it has high efficiency in inhibiting Al, density is less, the appearance is pleasing and corrosion resistant [5]. The inhibition of Al by organic compounds is as follows adsorbing organic particles on the metal surface and forming a protective layer which reduces metal corrosion [6-8]. Chemical and Physical adsorption are the two highest type of adsorption that occur as obtained data of interaction among organic inhibitors and the metal surface. The collection of these compounds is established on: a) are highly soluble in the examined medium, and b) contain polar functional groups (such as N=N, –CN, and C=O) and multiple bonds and c) have high molecular size

The objective of this work is to examine the protective action of HCD, as a safe-inhibitor, against the Al corrosion in 1.0 M HCl solution utilizing different tests such as ML and some electrochemical methods. The obtained data were verified by using FT-IR spectroscopy, AFM, SEM, and theoretical data.
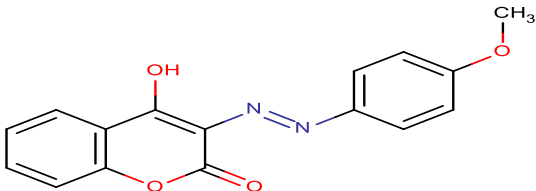
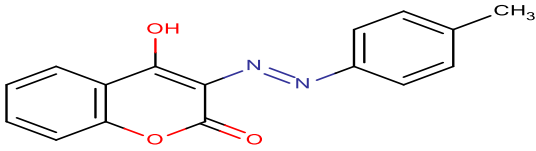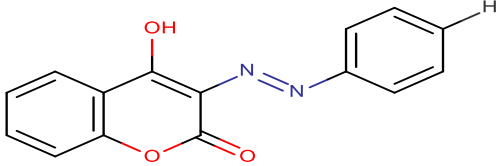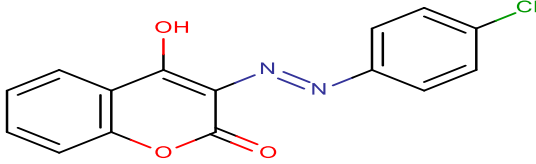## 2. MATERIALS AND TECHNIQUES

2.1. Materials and solutions

The working electrode was prepared from Al sheet (99.98%). The coins were mechanically abraded with dissimilar grades of emery papers (320- 2000) then wash away with twice distilled water, and desiccated at room temperature. The preparation of aggressive solution using twice distilled water to dilute analytical reagent grade 37% HCl to obtain the required acid concentration (1 M HCl).

2.2. Inhibitors

The investigated 4-hydroxycoumarin and its para-substituted derivatives were synthesized according to the procedures that illustrated in previous paper [9]. These compounds are presented in Table (1). The stock solutions of HCD (10^{-3}M) were ready by dissolving an accurately weight quantity of each material in suitable volume of dimethyl formamide (DMF) and absolute ethanol, then the required concentration (4×10^{-6} - 24×10^{-6}M) were prepared by dissolving with twice distilled water.

Table 1. Chemical structures and molecular formulas of the organic inhibitors

Comp	Structures	Names	Mol. Formulas, Mol. Weights
A		4-hydroxy-3-(p-methoxyphenylazo)-benzopyrane-2-one	$C_{16}H_{12}N_2O_4$ 296.28

B		4-hydroxy-3-(p-methyl phenylazo)-benzopyrane-2-one	$C_{16}H_{12}N_2O_3$ 280.28
C		4-hydroxy-3-phenylazo-benzopyrane-2-one	$C_{15}H_{10}N_2O_3$ 266.25
D		4-hydroxy-3-(p-chloro-phenylazo)-benzopyrane-2-one	$C_{15}H_9N_2O_3Cl$ 300.70

2.3. Techniques utilized for corrosion tests

2.3.1. Mass loss technique

Glass beaker of volume 100 ml was used in this method. The temperature of the experiment was controlled by using water bath. The Al pieces were prepared as previously mentioned. The solutions of 100 ml of 1M HCl only and with presence of various concentrations of HCD were prepared by immersion of Al coins for 3 hours at temperature range from 25 to 45°C. After every 30 min of the test the Al was detached from the solution, washed with twice distilled water, dried and then weighed carefully by sensitive balance. The (I %) and surface coverage (θ) could be measured from the average ML values as in the next eq. (1).

$$I \% = \Theta \times 100 = [\, 1 - (W_{inh} / W_{free})] \times 100 \qquad (1)$$

where W_{free} is the average ML of Al in acid only and W_{inh} of acid in presence of different concentrations of HCD.

2.3.1.1 Temperature Effect

The influence of temperature on the Al corrosion was studied at various temperatures as 25°C, 30°C, 35°C, 40°C and 45°C for 3 hours. The results obtained from this study could be used to calculate the (I %), activation and adsorption parameters.

2.3.3 Electrochemical procedures

The electrochemical cell, which utilized in the experiments, consists from three electrodes. These electrodes are reference electrode which is calomel electrode, the auxiliary electrode and Al electrode. The Al electrode was designed to make $1cm^2$ from the outer Al surface area exposed to the corrosive acid. Computer containing Gamry instrument Potentiostat/Galvanostat was utilized to

measure the corrosion rate by two different techniques (Tafel polarization, EFM and EIS). This computer was utilized to collect the results by Gamry applications, which contain EIS300 for EIS, DC105 for polarization and EFM140 for (EFM) tests. Graph and fit data were done by using software like Echem Analyst. The electrode potential was automatically changed from (-0.8 to 0.8 V vs. SCE) at OCP with a scan rate 1 mVs^{-1} to obtain Tafel polarization diagrams. The corrosion current densities could be obtained by extrapolation of the cathodic and anodic diagrams to corrosion potential. The (I %) and (Θ) were measured by utilizing corrosion current density (i$_{corr}$) according to the following eq. (2).

$$I\% = \Theta \times 100 = [1 - (i_{corr(inh)} / i_{corr(free)})] \times 100, \qquad (2)$$

where i$_{corr(free)}$ is the corrosion current density for Al in acid only and i$_{corr(inh)}$ for Al in acid with various concentrations of inhibitor.

EIS technique was carried out in suitable conditions such as frequency range of 10^7 Hz to 0.1 Hz with amplitude of 5 mV [10]. According to the next eq. (3), the (I %) and (Θ) were measured by utilizing the next eq. (3)

$$I\% = [1 - (R^{\circ}_{ct} / R_{ct})] \times 100 = \Theta \times 100, \qquad (3)$$

where R°_{ct} and R_{ct} represent the resistance of charge transfer for Al in acid only and with presence of various concentrations of inhibitor.

Two frequencies: 2 and 5 Hz were used in EFM test. Three evidences are the principles for the choice of these frequencies [11-13]. The parameters obtained from EFM (i$_{corr}$, ß$_a$, ß$_c$ and the causality factors CF-2&CF-3 were measured by using the large peaks. Before any measurements, the electrode potential was allowed to stabilize half hour. The electrochemical processes were done at room temperature.

2.4 Surface characterization

The Al metal was put in 1M hydrochloric acid only and in acid with addition of higher concentration of HCD for 24 hours, removed from the solution and dried at room temperature. The film formed on the Al surface was examined by using techniques such as SEM, AFM and FT-IR spectroscopy.

2.5 Quantum Chemical Calculations

Using PM3 semi-empirical method to optimize the molecular structure of the HCD to speed up the calculations. Density function theory (DFT) re-optimized resulting optimized structures using the GGA/BOP basis set. Quantum chemical measurements were performed utilizing DMol^3 module in Materials Studio v. 6.0.

3. RESULTS AND DISCUSSION

3.1. Tafel polarization (TP) characterization
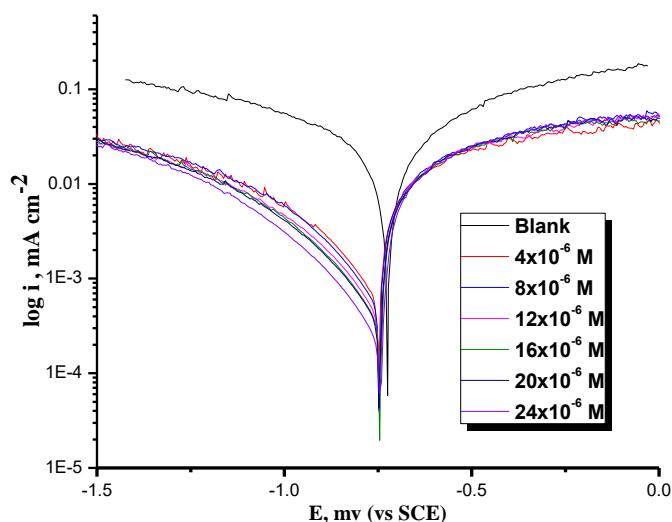
Figure 1. Tafel polarization graphs for Al corrosion in with and without various concentrations of compound A at 25°C

Table 2. TP parameters at various concentrations of investigated compounds on Al corrosion in 1M HCl at 25°C

| Comp	Conc., x10^6 M 10^6 M	i_{corr}, μA cm^{-2}	- E_{corr}, mV vs SCE	β_a mV dec^{-1}	β_c mV dec^{-1}	C.Rx10^2 mpy	Θ	% I
Blank	0.0	510	735	120	257	154	--	--
A	4	67.8	770	80	160	70	0.778	77.8
	8	58.5	740	78	140	69	0.802	80.2
	12	55.30	742	71	143	52	0.853	85.3
	16	40.6	753	67	133	22	0.873	87.3
	20	26.2	752	68	129	15	0.916	91.6
	24	21.5	754	70	137	10	0.935	93.5
B	4	79.3	740	88	158	88	0.759	75.9
	8	67.8	770	83	152	71	0.775	77.5
	12	61.00	742	76	139	62	0.827	82.7
	16	51.7	755	73	144	32	0.867	86.7
	20	33	762	67	133	28	0.902	90.2
	24	26.2	763	72	131	18	0.924	92.4
C	4	81.5	771	74	166	94	0.739	73.9
	8	73.5	766	88	140	81	0.755	75.5
	12	68.60	770	76	137	72	0.808	80.8
	16	56.3	770	79	151	42	0.847	84.7
	20	37.7	754	77	142	38	0.878	87.8
	24	28.4	763	74	138	25	0.904	90.4
D	4	81.5	771	84	144	98	0.718	71.8
	8	73.5	766	85	140	86	0.733	73.3
	12	68.60	770	76	155	79	0.784	78.4
	16	56.3	770	81	139	52	0.808	80.8
	20	37.7	754	84	142	48	0.849	84.9
	24	28.4	763	81	128	35	0.886	88.6

Figure 1 indicates the resulting effect on TP graphs for Al corrosion in 1M hydrochloric acid only and also in acid in existence of varied concentrations of the inhibitor (A). Other curves were received for other compounds (not presented). Parameters that related to this processes were listed in Table 2. It was observed that the data of i_{corr} decrease gradually in presence of HCD inhibitors and hence decreases the corrosion rate. Both anodic and cathodic diagrams move to lower current density in existence of inhibitors in 1M hydrochloric acid. It was found that the mechanism of Al corrosion process and hydrogen evolution not change when inhibitors were added. This is due to the stability values of both anodic and cathodic slopes in presence of HCD. Generally, if the E_{corr} in presence of inhibitors move to more 85 mV than in case of absence of inhibitor, this inhibitor will be classified as cathodic type [14]. In presence of HCD, corrosion potential (E_{corr}) transmits to negative value but this move is less than 85 mV, so these compounds can be classified as mixed kind inhibitors. The order of IE of the investigated inhibitors is observed to be: A > B > C > D

3.2. EIS Characterization

Both Nyquist and Bode graphs for Al corrosion in 1M HCl only and also in acid in presence of various concentrations of inhibitor (A) were obtained by EIS procedure and shown in Figures 2. The same curves attained for other compounds (not presented). It is noticed from Nyquist Figure that the curves appear semicircular.
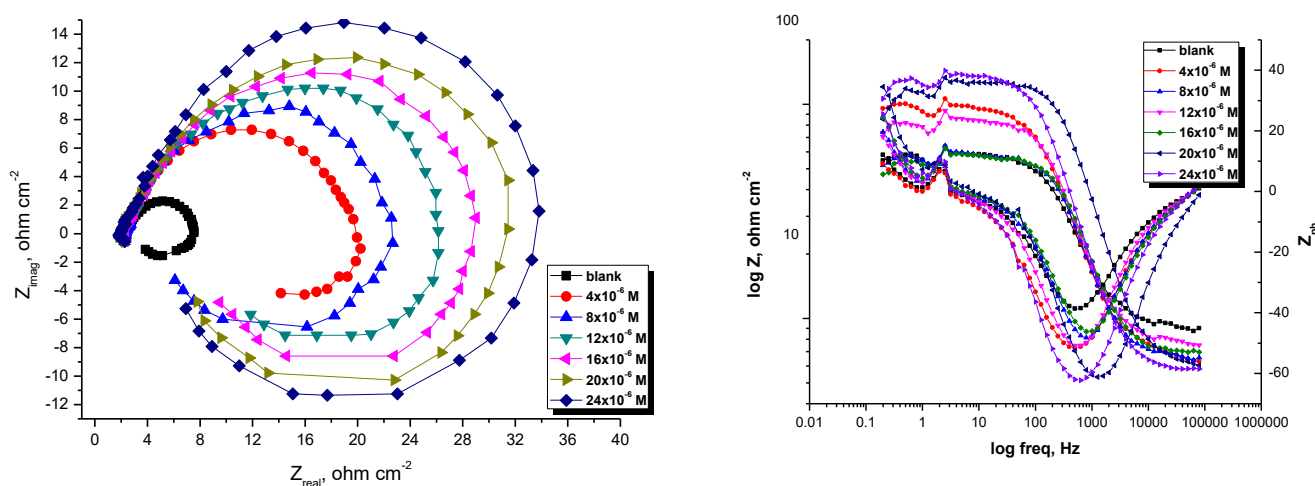
Figure 2. Nyquist and Bode graphs for Al corrosion in 1M HCl only and in acid in existence of varied concentrations of inhibitor (A) at 25°C
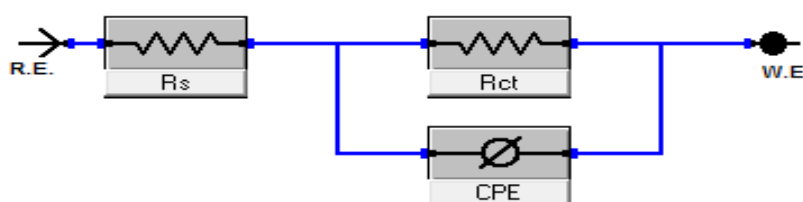
Figure 3. Circuit utilized to model impedance data in 1M HCl solutions

The frequency dispersion is responsible for the shape of the curves. The special shape of the Nyquist curves confirms that the Al corrosion is controlled by charge transfer process [15, 16]. It was found that in the Nyquist diagrams the presence of inhibitor leads to increase the diameter of capacitive loop. Resistance of charge transfer (R_{ct}) is responsible for high frequency capacitive loop. Figure 3, which represent a single charge transfer reaction and fits well with our experimental result data. The constant phase element, CPE, is introduced in the circuit instead of a pure double layer capacitor to obtain a more correct fit [17]. The (C_{dl}) is the frequency at which the element of the impedance is maximum and could be measured according to the next eq. (4)

$$C_{dl} = 1 / 2\, \pi\, F_{max}\, R_{ct} \tag{4}$$

where R_{ct} is the charge transfer resistance and F_{max} is the frequency at the maximum height of the semicircle [18,19]. To measure the (I %), eq. (3) was applied. The parameters obtained by EIS process was reported in Table 3.

Table 3. Parameters obtained by EIS process for Al corrosion in 1M HCl only (blank) and in acid in existence of varied concentrations of examined compounds at 25°C

Comp	Conc., x 10^6 M	R_{ct}, Ω cm^2	C_{dl},x10^{-3} μFcm^{-2}	θ	%I
Blank	0	2.1	190	---	---
A	4	8.1	110	0.741	74.1
	8	11.3	100	0.814	81.4
	12	13.8	90	0.848	84.8
	16	16.2	80	0.870	87.0
	20	19.9	60	0.894	89.4
	24	29.1	40	0.928	92.8
B	4	7.4	120	0.716	71.6
	8	10.8	115	0.806	80.6
	12	11.2	111	0.812	81.2
	16	15.4	98	0.864	86.4
	20	16.0	80	0.868	86.8
	24	23.6	70	0.911	91.1
C	4	7.1	128	0.704	70.4
	8	8.9	122	0.764	76.4
	12	10.1	117	0.792	79.2
	16	13.1	105	0.840	84.0
	20	14.9	94	0.859	85.9
	24	21.4	83	0.902	90.2
D	4	6.1	133	0.656	65.6
	8	8.9	127	0.764	76.4
	12	9.6	120	0.781	78.1
	16	12.4	113	0.831	83.1
	20	13.7	105	0.847	84.7
	24	17.8	92	0.882	88.2

From the obtained data, it was observed that the R_{ct} values increase with increasing investigated compound concentration but C_{dl} values decrease. The results obtained prove that the HCD works by forming the protecting layer on the Al surface which changes the Al/acid interface. The order of IE obtained from EIS test is: A> B > C > D.

3.3. EFM characterization

Intermodulation spectrum was obtained from EFM experiments. The spectrum is due to current response as a function of frequency. The equivalent current response in intermodulation spectrum for Al corrosion in acidic solution only and also in acid in existence of varied concentrations of inhibitor (A) was shown in Figure 4. Similar intermodulation spectra were obtained for different compounds (not shown). Results obtained by EFM processes were shown in Table 4. EFM technique produces different corrosion parameters such as (I %), (β_a, β_c), (i_{cor}) and (CF-2, CF-3) for Al corrosion in hydrochloric acid in existence of varied concentrations of examined inhibitors. It was observed from obtained information that the corrosion current density data lower with improving the HCD concentration and hence the IE% rises.
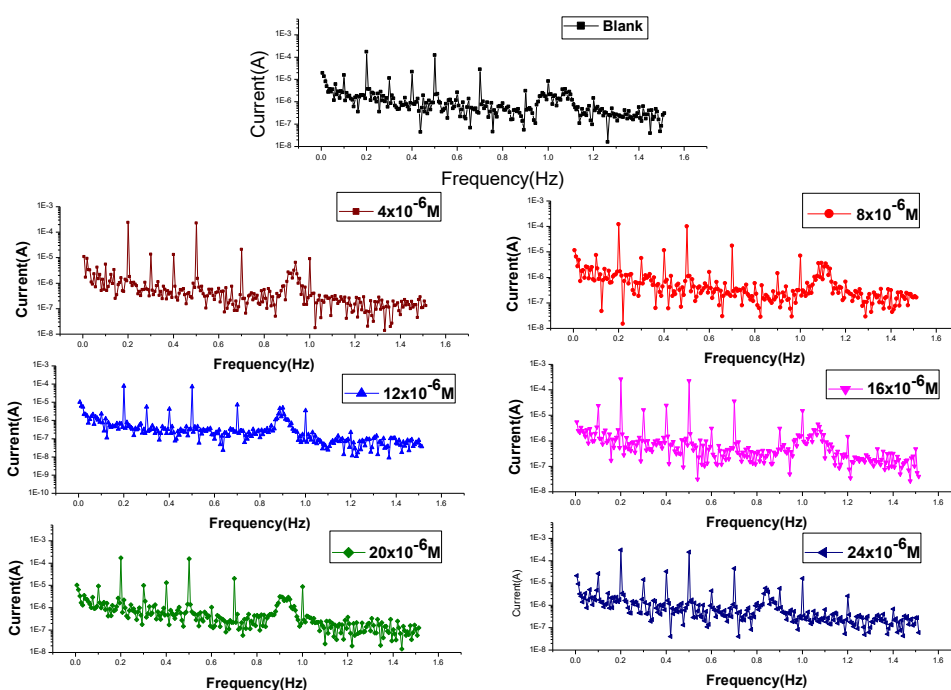
Figure 4. EFM spectra for Al corrosion in 1M hydrochloric acid only and also in acid in existence of varied concentrations of inhibitor (A) at 25°C

The data obtained showed that the causality factors values are very near to their theoretical values and this is very important to verify the corrosion current densities values and Tafel constants data according to EFM theory [20]. The causality factors obtained confirm the safety of the experiments. The normal values of CF-2 and CF-3 are about 2 and 3 correspondingly. The frequency

spectra of the current response were used to calculate the causality factors. If the EFM measurements were affected by noise, the causality factors would depart significantly from the theoretical values. If the causality factors are very near to the theoretical data, the results obtained are powerful data. The presence of the causality factors which act as quality control on the validity of the EFM makes this technique powerful. The % I that evaluated from this test is in the order A > B > C > D.

Table 4. Parameters obtained by EFM process for Al corrosion in 1M HCl only and also in acid in existence of varied concentrations of investigated compound at 25°C

Comp	Conc., x 10^6 M	i_{corr} ,μAcm^{-2}	β_a, mVdec^{-1}	β_c, mVdec^{-1}	C.Rx10^3 mpy	CF-2	CF-3	θ	%IE
Blank	0.0	574	152	210	677	2.1	3.1	---	---
A	4	160	120	150	230	1.9	3.0	0.721	72.1
	8	130	115	143	200	1.8	2.9	0.774	77.4
	12	120	110	132	190	2.3	3.1	0.791	79.1
	16	100	105	131	150	1.9	2.9	0.826	82.6
	20	51	99	125	142	1.8	3.3	0.911	91.1
	24	40	101	130	125	2.0	2.7	0.930	93.0
B	4	170	113	157	240	1.6	2.3	0.704	70.4
	8	140	108	149	215	1.8	2.7	0.756	75.6
	12	130	97	141	200	1.6	2.9	0.774	77.4
	16	110	93	137	165	1.7	2.6	0.808	80.8
	20	64	94	132	145	1.7	2.5	0.889	88.9
	24	47	96	124	138	2.0	3.0	0.918	91.8
C	4	183	107	164	250	2.2	3.2	0.681	68.1
	8	161	95	151	229	1.8	3.2	0.720	72.0
	12	140	91	148	205	2.1	2.7	0.756	75.6
	16	118	88	146	195	2.2	2.5	0.794	79.4
	20	76	94	137	160	2.0	3.3	0.868	86.8
	24	53	95	131	148	2.0	2.9	0.908	90.8
D	4	191	120	169	264	2.2	3.2	0.667	66.7
	8	177	118	157	233	1.8	3.2	0.692	69.2
	12	157	115	151	215	2.1	2.7	0.726	72.6
	16	125	111	149	201	2.2	2.5	0.782	78.2
	20	101	107	141	176	2.0	3.3	0.824	82.4
	24	66	99	139	161	2.0	2.9	0.885	88.5

3.4. ML characterization

The ML of Al samples in 1M HCl solution, in the existence and nonexistence various concentrations of the examined derivatives, was measured after 3 hours of inundation at 25 ±1°C. Figure 5 signifies this for compound (A) as an example. Similar diagrams were obtained for other compounds (not presented). Values of %I are given in Table 5 at various concentrations from the investigated compounds at 25°C.The results showed that the addition of HCD decrease the ML (mg

cm^{-2}) and the corrosion rate (C.R.). The (% I) and the θ, of the examined compounds for the corrosion of Al were calculated from eq. (1) [21]. % I occurred by these compounds decreased in the order: A > B > C > D.
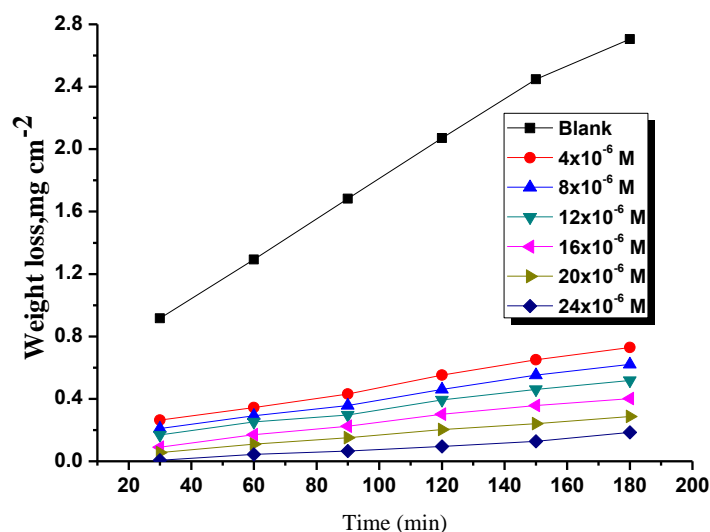
Figure 5. ML-time curves for the dissolution of Al without and with various concentrations of compound (A) at 25°C

Table 5. % I of all compounds at 120 min for Al corrosion in 1M HCl solution without and with various concentrations of investigated compounds as determined from ML technique at 25°C

Comp	A		B		C		D	
Conc., x 10^6 M	Θ	% I	Θ	% I	Θ	% I	Θ	% I
4	0.773	77.3	0.741	74.1	0.712	71.2	0.702	70.2
8	0.845	84.5	0.823	82.3	0.804	80.4	0.763	76.3
12	0.864	86.4	0.848	84.8	0.831	83.1	0.809	80.9
16	0.883	88.3	0.874	87.4	0.862	86.2	0.843	84.3
20	0.913	91.3	0.901	90.1	0.888	88.8	0.864	86.4
24	0.926	92.6	0.915	91.5	0.906	90.6	0.873	87.3

3.5. Effect of temperature

Various inhibitors concentrations were examine in the temperature range of 298–318 K utilizing ML tests. It was found that the % I decreases with raising temperature but at slight rate than in unprotected solutions with increasing the concentration of the HCD, as shown in Table 6, also the data from (Table 6) for compound (A), explains that the adsorption decreases with increasing the temperature and corrosion rate (k$_{corr}$) [22], similar tables were acquired for other compounds (not shown).

Figure 6 variation of I% of compound (A) with various temperatures using different concentrations of compound (A) for Al corrosion in 1M HCl, (similar curves were acquired in presence of the other compounds, (but not presented). The decrease of % I with temperature rise an indication for the physical adsorption of these investigated compounds on Al surface.
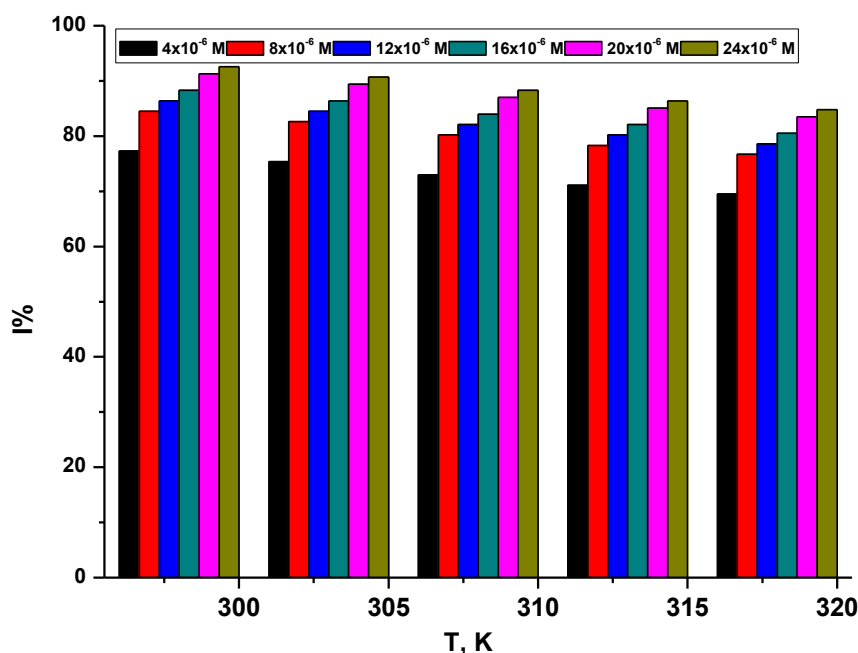
Figure 6. Effect of temperature on % I at various concentrations of compound (A) for Al corrosion in 1M HCl

Table 6. Values of % I, (θ) and corrosion rate (k_{corr}) for Al dissolution after 120 min immersion in 1M HCl without and with various concentrations of compound (A) at various temperatures

Conc., x 10^6 M	Temp, K	k_{corr}, mg cm^{-2} min^{-1}	θ	%I
blank		16.7	------	------
4		3.7	0.773	77.3
8		2.5	0.845	84.5
12		2.2	0.864	86.4
16		1.9	0.883	88.3
20	298	1.4	0.913	91.3
24		1.2	0.926	92.6
blank		18.3	----	-----
4		4.5	0.754	75.4
8		3.1	0.826	82.6
12		2.8	0.845	84.5
16	303	2.4	0.864	86.4
20		1.9	0.894	89.4
24		1.7	0.907	90.7

blank		22.4	-----	------
4		6.0	0.73	73
8		4.4	0.802	80.2
12		4.0	0.821	82.1
16	308	3.5	0.84	84
20		2.9	0.87	87
24		2.6	0.883	88.3
blank		44.5	------	------
4		12.8	0.711	71.1
8		9.6	0.783	78.3
12		8.8	0.802	80.2
16	313	7.9	0.821	82.1
20		6.6	0.851	85.1
24		6.0	0.864	86.4
blank		58.3	------	------
4		17.7	0.695	69.5
8		13.5	0.767	76.7
12	318	12.4	0.786	78.6
16		11.3	0.805	80.5
20		9.6	0.835	83.5
24		8.8	0.848	84.8

The (E^*_a) of the corrosion process was measured utilizing Arrhenius eq. (6):

$$k_{corr} = A \exp(-E^*_a / RT) \quad (6)$$

where A is Arrhenius constant and E^*_a values of activation energies. The E^*_a data can be result from the slope of the lines of drawing log k_{corr} vs 1/T (Figure 7) with and without investigated compounds at various temperatures, the data are given in Table 7. The E^*_a values increases in presence of inhibitor than in their absence. The measured E^*_a established that the examined compounds inhibit corrosion more effectually at upper concentrations. Likewise, improve in E^*_a with the presence of various concentrations of investigated compounds showing that the energy barrier for the corrosion reaction rises. These data showed that the existence of these HCD inhibitors improve the E^*_a of the metal dissolution reaction and that the process is diffusion controlled ($E^*_a > 40$ kJ mol^{-1}). The blocking of the active sites must be connect with rise in the E^*_a of Al corrosion in the protect state [23-24]. ΔH^* and ΔS^* are measured from transition state theory utilizing eq. (7) [25]:

$$k_{corr} = RT/Nh \exp(\Delta S^*/R) \exp(-\Delta H^*/RT) \quad (7)$$

where h is Planck's constant. Figure 8 displays a draw of log (k_{corr} /T) vs (1/T). Lines are achieved with a slope of ($\Delta H^*/2.303$ R) and an intercept of (log R/Nh + $\Delta S^*/2.303$ R) and with linear regression (R^2) is close to 1 from which the data of ΔH^* and ΔS^* are measured and also recorded in Table 7.

The enthalpy of a chemisorption process reached (100 kJ mol^{-1}) [26, 27]. The rise in the (ΔH^*) in existence of the inhibitors mean that the presence of these derivatives to 1M HCl solution rise the height of the energy barrier of the corrosion reaction to an extent depending on the concentration of the

existence of these compounds. The -ve ΔS^* showed that the activated complex in the rate-determining step signifies an association rather than dissociation step [28].
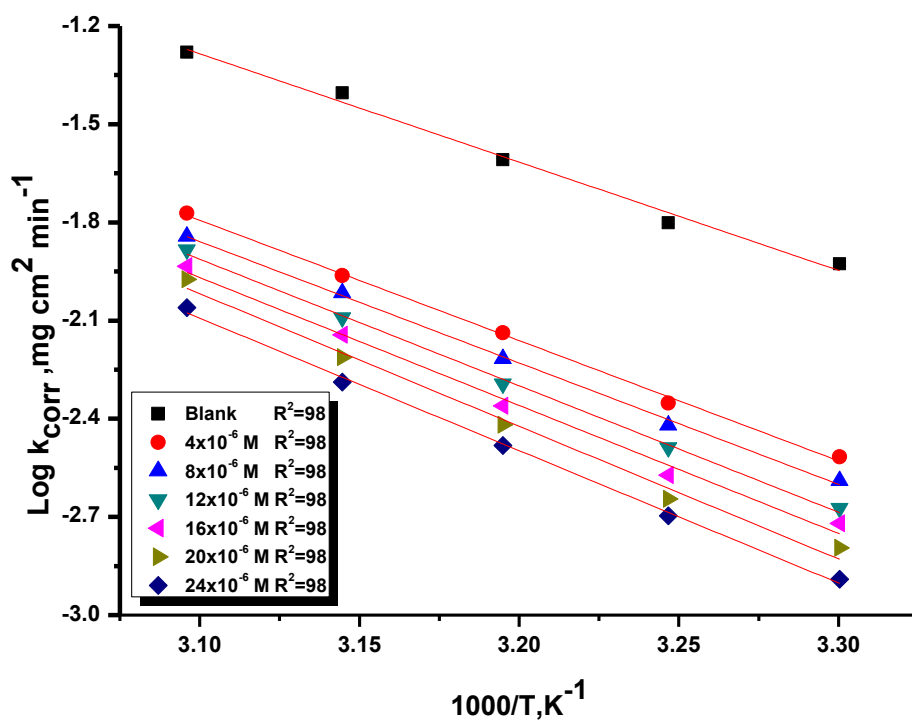
Figure 7. Arrhenius plots (log k_{corr} vs 1/T) for the dissolution of Al in 1M HCl without and with various concentrations of compound (A)
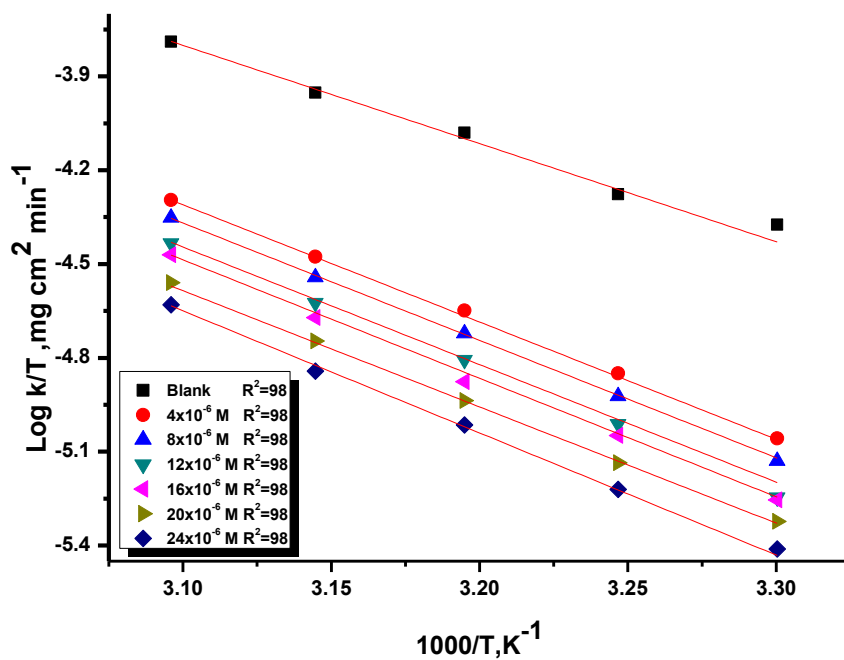
Figure 8. Plots of (log k_{corr} / T) vs 1/ T for the dissolution of Al in 1M HCl without and with various concentrations of compound (A)

Table 7. Kinetic activation data for Al corrosion in 1M HCl without and with various concentrations of all inhibitors

Comp	Conc., x 10^6 M	E_a^*, kJ mol^{-1}	ΔH^*, kJ mol^{-1}	$-\Delta S^*$, J mol^{-1}K^{-1}
Blank	0.0	61.4	58.8	84.6
A	4	72.4	69.8	79.6
	8	73	70.4	57.3
	12	73.1	70.5	56.8
	16	74.8	72.2	55.2
	20	76.1	73.5	54.3
	24	77.9	75.3	53.5
B	4	70.6	68	81.6
	8	71.8	69.2	61.4
	12	71.9	69.3	60.3
	16	73.2	70.6	59
	20	73.8	71.2	58.3
	24	76	73.4	58
C	4	66.6	64	82.5
	8	68.3	64.7	70.2
	12	69.2	65.8	64.2
	16	67.9	66.3	63.4
	20	67.2	67.6	62.3
	24	67.8	68	61.8
D	4	65.3	62.7	82.8
	8	65.6	63.4	77.2
	12	65.8	63.8	76.6
	16	66.2	64.3	75.6
	20	66.6	65.1	74.2
	24	66.9	65.9	73.1

3.7. Adsorption isotherms

Different isotherms were applied on the obtained data from several curves by fitting these results. Figure 9 shows the graphs between (C/Ө) and (C) concentration of inhibitor A. Alike diagrams were acquired for other compounds (not presented). These diagrams were straight lines and give the correlation coefficient equal approximately unity. The good value of correlation shows that the type of adsorption of inhibitor on Al surface is Langmuir isotherm. Consequence, it is illustrated that there is harmony among the adsorbed molecules on the Al surface [29]. The standard free energy of adsorption (ΔG°_{ads}) can be measured from the data of the equilibrium constant (K_{ads}). The constant (K_{ads}) of the adsorption can be measured by the next eqs. [30, 31]:

$$C/Ө = 1/K_{ads} + C \tag{8}$$

$$K_{ads} = 1/55.5 \exp(-\Delta G^\circ_{ads})/RT \tag{9}$$

where 55.5 expresses to the concentration of water species with unit (mol L^{-1}) at metal/solution interface

The thermodynamic parameters results obtained are shown in Table 8. From these results, it was found that the ΔG°_{ads} has negative sign. This -ve ΔG°_{ads} designates that the adsorption of investigated inhibitors on Al surface is spontaneous process.
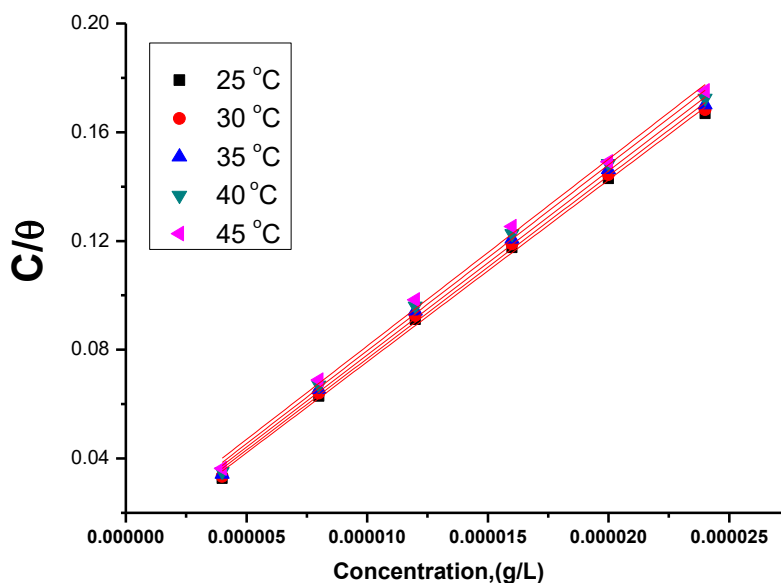
Figure 9. Diagrams from Langmuir for the adsorption of compound (A) on Al in 1M HCl at various temperatures
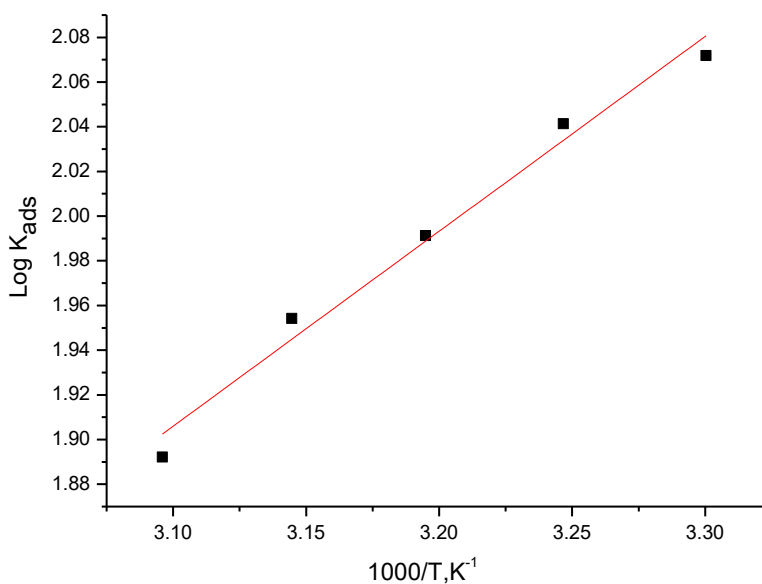
Figure 10. Van`t Hoff plots (Log K_{ads} vs 1/T) of inhibitor (A) in 1M HCl

In General, if the data of ΔG°_{ads} reached about -20 kJ mol^{-1}, there will be electrostatic interaction among the charged Al and the charged molecules and this type of adsorption is called physical adsorption. Also, if the values of ΔG°_{ads} reached more than -40 kJ mol^{-1}, there will be transfer of electrons from the inhibitor molecules to the Al surface and this type is called chemisorption [32, 33]. The Van't Hoff equation was utilized to calculate (ΔH°_{ads}) as follows [34]:

$$\ln K_{ads} = - \Delta H°_{ads} /RT+ const. \tag{10}$$

The graph between $\log K_{ads}$ and $1/T$ for Al degradation in 1M hydrochloric acid in presence of inhibitor (A) appears in Figure 10. From the results in Table 8, it is shown that the adsorption is an exothermic process due to the -ve sign $\Delta H°_{ads}$ [35, 36]. At the end, the standard adsorption entropy $\Delta S°_{ads}$ can be determined from the following eq.(11):

$$\Delta G°_{ads} = \Delta H°_{ads} - T \Delta S°_{ads} \tag{11}$$

From the calculated data in Table 8, it is appeared that the standard adsorption entropy data have negative sign. Negative value $\Delta S°_{ads}$ showed that a decrease in disorder of corrosion process on Al surface in 1M HCl using organic compounds as corrosion inhibitors (Table 8) [37,38].

Table 8. Thermodynamic parameters for Al corrosion in HCl for investigated compounds at various temperatures

Comp	Temp., K	K_{ads} M^{-1}	$-\Delta G°_{ads}$ kJ mol^{-1}	$-\Delta H°_{ads}$ kJ mol^{-1}	$-\Delta S°_{ads}$ J mol$^-$K^{-1}
A	298	125	22.1	26.1	71.2
	303	114	21.2		68.3
	308	101	20.3		66.1
	313	98	19.4		65.9
	318	77	18.5		63.1
B	298	75	20.6	30.7	69.1
	303	65	20.1		66.5
	308	60	19.6		63.3
	313	56	19.1		62.7
	318	47	18.1		61.8
C	298	44	18.4	32.2	66.2
	303	39	18.1		62.7
	308	36	17.9		61.3
	313	32	17.2		60.1
	318	26	16.9		58.3
D	298	35	17.9	36.7	61.2
	303	28	17.3		59.7
	308	27	16.8		57.4
	313	25	16.3		54.4
	318	21	15.9		51.2

3.8. Atomic force microscopy (AFM) analysis

AFM is very important technique to confirm the efficiency of the inhibitors on the metal surface. AFM technique gives roughness data for different surfaces which make this method powerful. The images produced from this method could be used to differentiate between several Al surfaces easily [39].
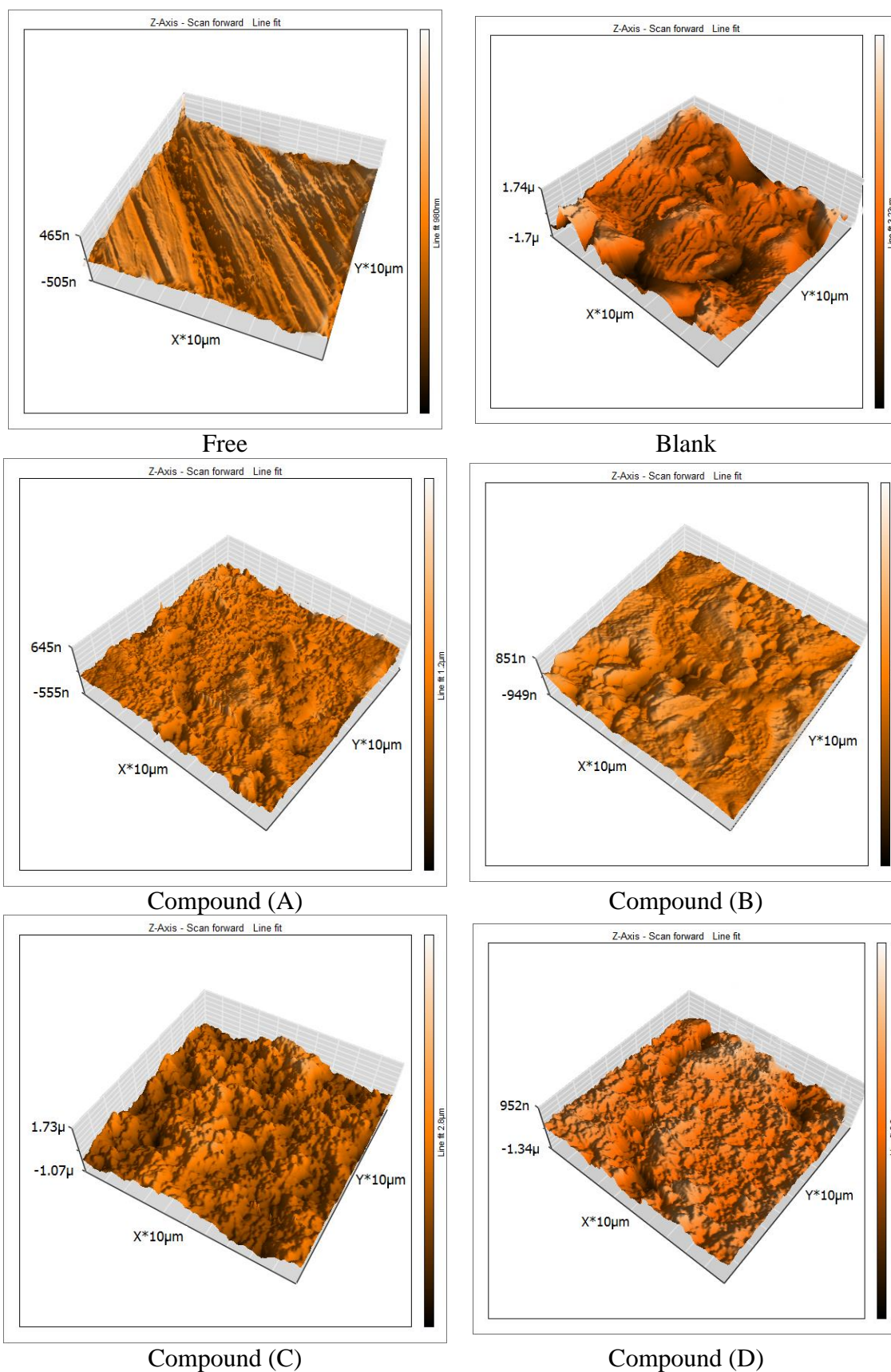
Figure 11. Three-dimensional (3D) AFM images Al metal before immersion in acid (free) Al metal immersion in 1M HCl alone (blank) and Al metal immersion in 1M HCl at 24×10^{-6} M of examined compounds (A-D) for 24 hours at 25°C

The 3D images for polished Al surface (standard specimen), Al immersed in 1M hydrochloric acid (blank) and Al immersed in 1M hydrochloric acid containing 24×10^{-6} M from investigated compounds were shown in Figure 11. Roughness data for different Al surfaces are listed in Table 9. The roughness data give clear indication that the Al surface appears smoother due to the adsorption of the inhibitors on its surface and creating the protective layer [40].

Table 9. AFM roughness data of compounds (A-D) at 24×10^{-6}M for 24 hours at 25°C

Specimen	Average roughness(**Sa**) nm
Free	33.2
Blank	433.5
compounds (A)	71.9
compounds (B)	83.4
compounds (C)	93.8
compounds (D)	121.3

3.9. (SEM) morphology
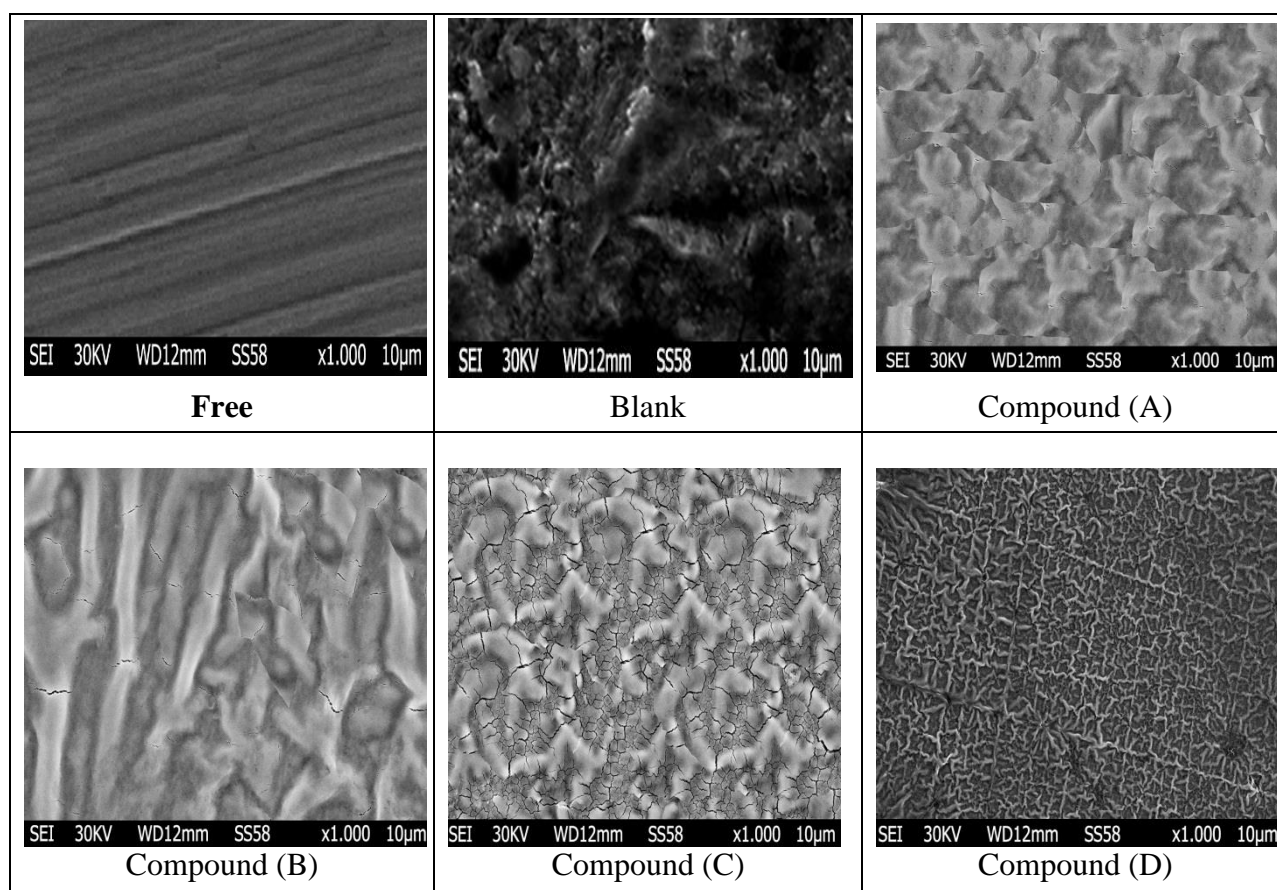
Figure 12. SEM images for Al in the with and without 24×10^{-6} M of examined compounds (A-D) after immersion for 24 hours at 25°C

To estimate the changes of the metal surface immersed in acid solution with and without inhibitors (A-D). The Al surface was analyzed using SEM. The Al samples in 1.0 M HCl solution in the presence and absence of the highest concentration of the inhibitors (A-D) (24×10^{-6}) for one day were exposed to analysis. Figure (12) shows SEM micrographs. It is clear that, Al surface corrosion was reduced with the presence of the inhibitors (A-D). The other pictures revealed that there is high damage, several pits and cavities on the Al surface in the absence of inhibitors (A-D). This may be due to the adsorption of the organic compounds on the Al surface and create the passive film on it, this blocks the active sites existence on the Al surface [41, 42].

3.10. FTIR examination

Functional groups and characterizing covalent bonding data had been noticed by FT-IR which is significant analytical device [32] FTIR spectrum of the corrosion creation at Al superficial in 1M HCl does not display any suitable adsorption peaks; therefore, the corrosion creation of Al is not IR active. The finger print spectra of the inhibitor (A) and the Al surface after immersion in 1M HCl + 24×10^{-6} M of inhibitor A for 6 hours was give and associated to each other it was clearly clear that the same finger print of inhibitor (A) stock solution existence on Al surface except the nonexistence of some functional group and it recommended due to reaction with HCl. (similar plots were obtained in existence of the other compounds, (but not presented). From Figure 13 there are minor shift in the peaks at Al superficial from the original peak of the stock inhibitor solution, these changes designate that there is interaction among Al and HCD inhibitor's molecules.
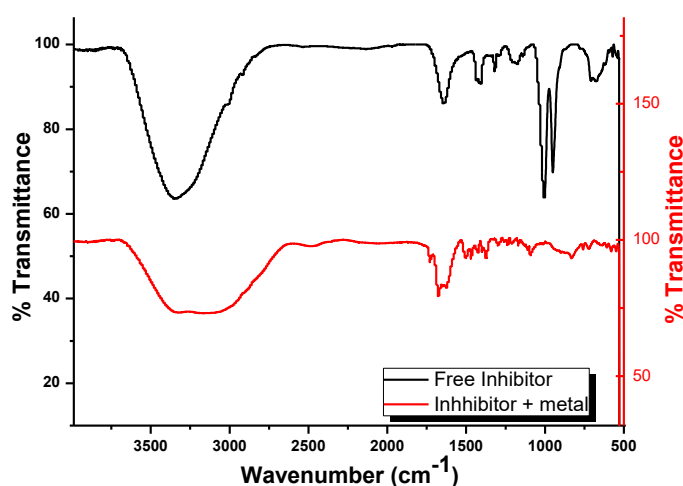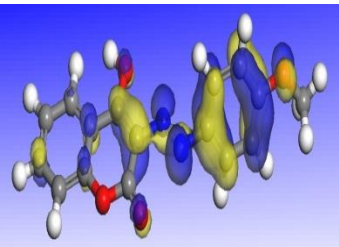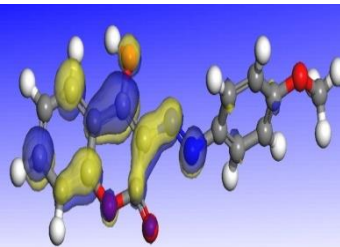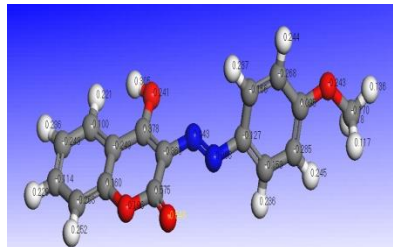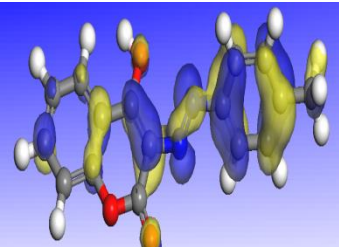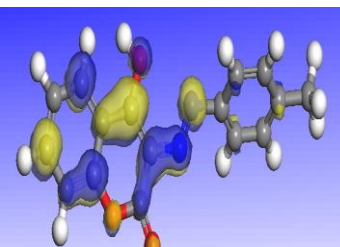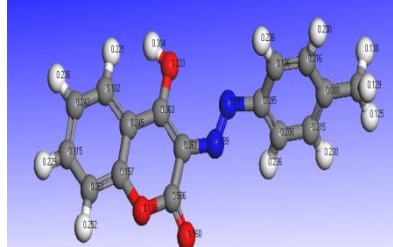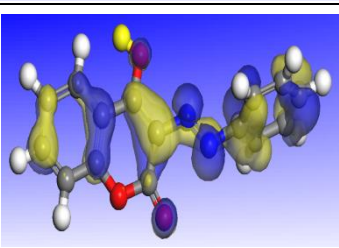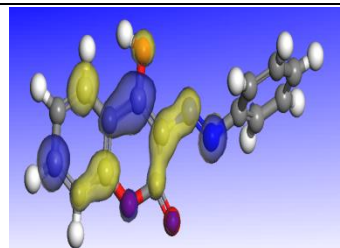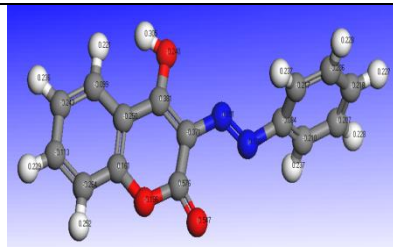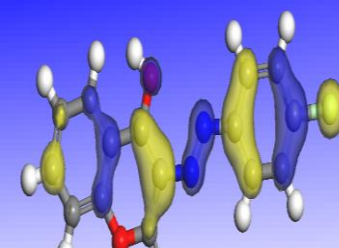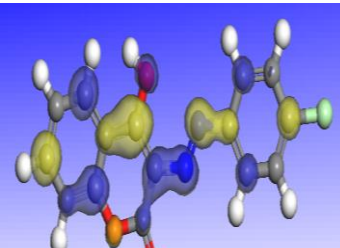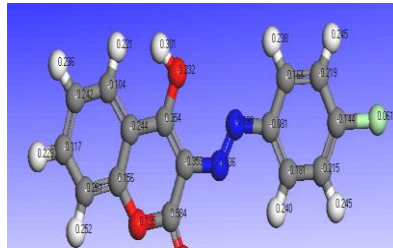

Figure 13. FTIR spectra of inhibitor (A) stock solution (10^{-3} M) (b) and adsorbed layer of inhibitor (A) on Al surface (a)

3.11. Theoretical study of inhibitors

The measured quantum chemical directories (E_{HOMO}, E_{LUMO}, μ) of examined composites are displayed in Table 10. The variance $\Delta E = E_{LUMO} - E_{HOMO}$ is the energy need to move an electron from

HOMO to LUMO. (ΔE), which is significant constancy index, is useful to improve theoretical models for elucidation the structure and conformation barriers in many molecular systems [43, 44]. The smaller is the data of ΔE, the more is the probable protection efficiency. It was displayed from Table 10 that compound (A) has the lowest (E_{LUMO}–E_{HOMO}) energy gap related with the other molecules.

Inhibitors	HOMO	LUMO	Mulliken Charges
A			
B			
C			
D			

Figure 14. The frontier molecular orbital density distribution of the examined inhibitors (HOMO and LUMO).

Accordingly, it could be predictable that composite (A) has more inclination to adsorb on the A surface than the other molecules. The higher data of (μ), the more is the likely protection efficiency. Finally, from Table 10, we create that the E $_{HOMO}$ and the E $_{LUMO}$ exchanged regularly, while the ΔE lower with improving the protection efficiency(% I). The %I is associated with the exchanges of the E_{HOMO} and E_{LUMO}, which recommended that the inhibitors were maybe either the acceptor or the donor

of the electron. That is, there was electron transferring in the interaction among the inhibitor molecules and the Al surface. The ΔE lower with improving the % I, this designates that the more unstable of the inhibitors, the stronger interaction among the HCD and surface of Al. From the outcome data given we create that, the order of dipole moment lower in the next sequence:

Compound (A) > (B) > (C) > (D) and this approve with the outcome data gotten from the experimental tests.

Table 10. Quantum chemical parameter for investigated derivatives

Compounds	A	B	C	D
E_{HOMO}, (eV)	-9.18	-9.35	-9.47	-9.51
E_{LUMO}, (eV)	-1.42	-1.43	-1.44	-1.28
ΔE, (eV)	7.76	7.92	8.03	8.23
μ , (Debye)	-5.3	-5.4	-5.43	-5.46

4. MECHANISM OF CORROSION PROTECTION

As known from literature, the Al surface is negatively charged in acidic solutions [45]. These investigated compounds are present as protonated species (cationic form) in acid solution. So, it is easier for the protonated species to approach the negatively charged Al surface due to the electrostatic attraction [45]. Thus, we can achieve that protection of Al corrosion in HCl is mainly due to electrostatic interaction. The order of decreasing %I of the HCD compounds from all tests utilized techniques is: A > B > C > D. Inhibitor (A) is the most efficient inhibitor due to: i) the existence of greatly electron donatingp-OCH$_3$ group (with Hammett constant σ = -0.27) [46] which improves the delocalized π-electrons on the molecule ii) also may add an additional active site to the molecule due to its oxygen atom. Inhibitor (B) comes after inhibitor (A) in %I due existence of p-CH3 with (σ = -0.17) which contribute less electron density to the molecule and also the absence of oxygen atom so gives less active centers. Inhibitor (C) is the least efficient inhibitor, this may be due to the existence of substituent group in para position and existence of H atom (σ = 0.0) that donates no charge density to the molecule. Inhibitor (D) is the least efficient one, due to the presence of p-Cl (+0.22) group which acts as electron withdrawing groups; so it lowers the electron density on the active site and also the protection efficiency.

5. CONCLUSIONS

The examined composites show best performance as corrosion protection in HCl solution. The %I of 4-hydroxycoumarin derivatives follows the order: A > B > C > D. PP data displayed that HCD

perform as mixed kind inhibitors for Al in HCl solution. EIS studies led to R_{ct} data improved, while C_{dl} data lowered in the existence of the inhibitors. The adsorption of the examined inhibitors was established to obey the adsorption Langmuir isotherm indicating that the inhibition process occurs via adsorption. The attendance of the protective film on the surface of Al was proving by AFM, SEM and FTIR analysis. The %I obtained from electrochemical and non-electrochemical tests are in a best agreement.

References

1. K. C. Emregul and A.A. Aksut, *Corros. Sci*., 42 (2008) 2051.
2. M.G. Fontana and R.W. Staehle (Eds.), *Adv. Corros. Sci. Technol.*, 1 (1970) 248.
3. T. Jain, R. Chowdhary and S.P. Mathur, *Mater. Corros*., 57 (2006) 422.
4. S.L. Granese, *Corrosion*, 44 (1988) 322.
5. T. Mimani, S.M. Mayanna and N. Munichandraiah, *J. Appl. Electrochem*., 23 (1993) 339.
6. E.E. Oguzie, *Corros. Sci*., 49 (2007) 1527.
7. M.A. Hukovic, Z. Gribac and E.S. Lisac, *Corrosion*, 50 (1994) 146.
8. S.S. Mahmoud and G.A. El-Mahdy, *Corrosion*, 53 (1997) 437.
9. A.G.F. Shoair, *J. Coord. Chem.*, 60(10) (2007) 1101.
10. H. Ma, S. Chen, L. Niu, S. Zhao, S. Li and D. Li, *J. Appl. Electrochem.*, 32 (2002) 65.
11. R.W. Bosch, J. Hubrecht, W.F. Bogaerts and B.C. Syrett, *Corrosion*, 57 (2001) 60.
12. S.S. Abdel–Rehim, K.F. Khaled and N.S. Abd–Elshafi, *Electrochim. Acta*, 51 (2006) 3269.
13. Z. Khiati, A.A. Othman, M. Sanchez-Moreno, M.C. Bernard, S. Joiret, E.M.M Sutter and V. Vivier, *Corros. Sci*., 35 (2011) 3092.
14. W.H. Smyrl, J.O.M. Bockris, B.E.Conway, E. Yeager and R.E. White (Eds.), *Comprehensive Treatise of Electrochemistry, Plenum Press, New York,* 4 (1981) 116.
15. M. El–Achouri, S. Kertit, H.M. Gouttaya, B. Nciri, Y. Bensouda, L. Pere, M. Rinfante and K. Elkacemi, *Prog. Org. Coat.*, 43 (2001) 267.
16. J.R. Macdonald, W.B. Johanson, J.R. Macdonald (Ed.), John Wiley& Sons, *Fundamentals of impedance spectroscopy, book chapter 1, New York* (1987) 1.
17. S.F. Mertens, C. Xhoffer, B.C. Decooman and E. Temmerman, *Corrosion*, 53 (1997) 381.
18. M. Lagrenée, B. Mernari, M. Bouanis, M. Traisnel and F. Bentiss, *Corros. Sci*., 44 (2002) 573.
19. F. Bentiss, M. Lagrenée, and M. Traisnel, *Corrosion*, 56 (2000) 733.
20. E. Kus and F. Mansfeld, *Corros. Sci.*, 48 (2006) 965.
21. D.Q. Zhang, Q.R. Cai, X.M. He, L.X. Gao and G.S. Kim, *Mater. Chem. Phys*., 114 (2009) 612.
22. M.P. Chakravarthy, K.N. and C.P. Kumar, *Int. J. Ind. Chem.*, 5(2) (2014) 19.
23. A.S. Fouda, W.M. Mahmoud and K.M. A. Elawayeb, *Protection of Metals and Physical Chemistry of Surfaces,* 53(1) (2017) 13.
24. S.H. Etaiw, M.M. El-bendary, A.S. Fouda and M.M. Maher, *Protection of Metals and Physical Chemistry of Surfaces,* 53(5) (2017) 937.
25. A.S. Fouda, R.M. Abou Shahba, A.E. EL-Shenawy and T.J.A. Seyam, *Chem. Sci. Trans.,* 7(2) (2018) 1.
26. S.T. Arab and E.A. Noor, *Corrosion*, 49 (1993) 122.
27. W. Durnie, R.D. Marco, A. Jefferson and B. Kinsella, *J. Electrochem. Soc*., 146 (1999) 1751.
28. M.K. Gomma and M.H. Wahdan, *Mater. Chem. Phys*., 39 (1995) 209.
29. E. Khamis, *Corrosion*, 46 (1990) 476.
30. A.S. Fouda, A.M. El-desoky and A. Nabih, *Advances in Materials and Corrosion*, 2 (2013) 9.
31. A.N. Frumkin, *Zeitschrift für Physikalische Chemie*, 116 (1925) 466.
32. F. Bensajjay, S. Alehyen, M. El Achouri and S. Kertit, *Anti-Corros. Meth. Mater*., 50 (2003) 402.

33. L. Tang, X. Li, Y. Si, G. Mu and G. Liu, *Mater. Chem. Phys*., 95 (2006) 29.
34. A.K. Maayta and N.A.F. Al-Rawashdeh*, Corros. Sci.*, 46 (2004) 1129.
35. S.S. Abd El-Rehim, S.A.M. Refaey, F. Taha, M.B. Saleh and R.A. Ahmed, *J. Appl. Electrochem*., (2001) 429.
36. A.S. Fouda, D. Mekkia and A.H. Badr, *J. Korean Chem. Soc*., 57 (2013) 264.
37. X. Li and G. Mu, *Appl. Surf. Sci*., 252 (2005) 1254.
38. G. Mu, X. Li and G. Liu, *Corros. Sci.*, 47 (2005) 1932.
39. B. Wang, M. Du, J. Zang and C.J. Gao, *Corros. Sci.*, 53 (2011) 353.
40. S. Rajendran, C. Thangavelu and G. Annamalai, *J. Chem. Pharm. Res*., 4 (2012) 4836.
41. A.S. Fouda, Y.M. Abdallah and D. Nabil*, IJIRSET*, 3 (2014) 12965.
42. Y.Y. Enriadi and N.J. Gunawarman, *BCES*, 14 (2014) 15.
43. J.M. Costa and J.M. Liuch, *J. Corros. Sci*., 24 (1984) 929.
44. C. Lee, W. Yang and R.G. Parr, *Phys. Rev*. B, 37 (1988) 785.
45. L.R. Chauhan and G. Gunasekaran, *Corros. Sci*., 49 (2007) 1143.
46. H. Ashassi-Sorkhabi, B. Shaabani and D. Seifzadeh, *Appl. Surf. Sci*., 239 (2005) 154.